Low coverage genomic data resolve the population divergence and gene flow history of an Australian rain forest fig wasp

Lisa Cooper[1#], Lynsey Bunnefeld[2#], Jack Hearn[1,3], James M Cook[4], Konrad Lohse[1*], Graham N. Stone[1*].

1. Institute of Evolutionary Biology, University of Edinburgh, EH9 3FL Edinburgh, UK.

2. Biological & Environmental Sciences, University of Stirling FK9 4LA Stirling, UK.

3. Vector Biology Department, Liverpool School of Tropical Medicine, Liverpool, UK.

4. Hawkesbury Institute for the Environment, Hawkesbury Campus, Western Sydney University, Richmond, New South Wales, Australia

Corresponding author: Prof. Graham N. Stone, Institute of Evolutionary Biology, Charlotte Auerbach Road, University of Edinburgh, EH9 3FL Edinburgh, UK.

email: graham.stone@ed.ac.uk

# these authors are joint first authors of the paper

* these authors contributed equally to this work.

Key words: Demography, phylogeography, Australia, *Ficus, Pleistodontes,* Agaonidae.

Running title: Population divergence and gene flow in a fig wasp

Orcid identifiers:
L. Bunnefeld: 0000-0002-9226-7153
J.M. Cook: 0000-0001-8447-6126
J. Hearn: 0000-0003-3358-4949
K. Lohse: 0000-0001-9918-058X
G.N. Stone: 0000-0002-2737-696X

Abstract

Population divergence and gene flow are key processes in evolution and ecology. Model-based analysis of genome-wide datasets allows discrimination between alternative scenarios for these processes even in non-model taxa. We used two complementary approaches (one based on the blockwise site frequency spectrum (bSFS), the second on the Pairwise Sequentially Markovian Coalescent (PSMC)) to infer the divergence history of a fig wasp, *Pleistodontes nigriventris.* *Pleistodontes nigriventris* and its fig tree mutualist *Ficus watkinsiana* are restricted to rain forest patches along the eastern coast of Australia, and are separated into northern and southern populations by two dry forest corridors (the Burdekin and St. Lawrence Gaps). We generated whole genome sequence data for two haploid males per population and used the bSFS approach to infer the timing of divergence between northern and southern populations of *P. nigriventris,* and to discriminate between alternative isolation with migration (IM) and instantaneous admixture (ADM) models of post divergence gene flow. *Pleistodontes nigriventris* has low genetic diversity (π = 0.0008), to our knowledge one of the lowest estimates reported for a sexually reproducing arthropod. We find strongest support for an ADM model in which the two populations diverged *ca*. 196kya in the late Pleistocene, with almost 25% of northern lineages introduced from the south during an admixture event *ca.* 57kya. This divergence history is highly concordant with individual population demographies inferred from each pair of haploid males using PSMC. Our analysis illustrates the inferences possible with genome-level data for small population samples of tiny, non-model organisms and adds to a growing body of knowledge on the population structure of Australian rain forest taxa.

Introduction

Division of an ancestral population into daughter populations is a universal and repeating process in biology. The tempo and mode of population divergence are central to evolutionary

processes ranging from local adaptation and range expansion to the origin of species (Hey & Nielsen 2004; Martin et al., 2013; Sousa & Hey, 2013). From a demographic perspective, population divergence can be described in terms of the sizes of ancestral and descendant populations, the time at which the ancestral population split, and parameters capturing the timing, extent and direction of gene flow between descendant populations. Gene flow can be modelled in at least two general ways (Fig. 1): an isolation with migration (IM) model identifies gene flow as the result of ongoing dispersal (Nielsen & Wakeley 2001, Hey, & Nielsen 2004, Lohse et al 2011), while an instantaneous admixture (ADM) model associates gene flow with one or more discrete dispersal events in the past (Durand et al., 2011; Sousa & Hey, 2013; Lohse & Frantz, 2014). Thus, which of these models applies may tell us whether putative dispersal barriers are past or ongoing, and help to identify evolutionarily independent conservation units within species. The models also have very different implications for local adaptation: while local adaptation may proceed unimpeded during periods of complete isolation in the ADM model, continuous gene flow under the IM model imposes a constant genetic load of locally deleterious variants (Bisschop et al 2020).

Discriminating among alternative models of gene flow and estimating the relevant demographic parameters is a data-hungry problem and a growing number of approaches exploit the signal contained in whole genome data (WGD) for a small samples of individuals (Li & Durbin, 2011; Lohse & Frantz 2014; Bunnefeld et al., 2018). The falling costs of genome sequencing have made demographic inferences possible for rare and non-model taxa. Here we use two such approaches to infer the population divergence history of *Pleistodontes nigriventris*, a wasp that is the only pollinator of an endemic fig species (*Ficus watkinsiana*) found in two widely separated blocks of rainforest along the east coast of Australia (see below) (Dixon 2003; Lopez-Vaamonde et al., 2002). Our overall objective is to infer the extent and direction of fig wasp gene flow between these two populations, using WGD for just two individuals per population. Our approaches take advantage of the haplodiploidy of the Hymenoptera, by sampling males whose haploid genomes facilitate data analysis and interpretation.

We first compare support for alternative IM and ADM models using a parametric maximum-composite likelihood method (Lohse et al., 2011; 2016), and then compare these results with those obtained using the Pairwise Sequentially Markovian Coalescent (PSMC) (Li & Durbin, 2011), a non-parametric method. We chose these methods because they infer population history based on different aspects of genome-wide sequence variation, and have contrasting limitations. The Lohse et al. (2011) method is based on a blockwise summary of sequence variation, while PSMC exploits the information contained in the density of pairwise differences along a minimal sample of two haploid genomes. The Lohse et al. (2011) method – by design – lacks power to detect very gradual demographic changes (for example, in population size), while PSMC is known to smooth out very sudden changes (Li & Durbin, 2011). The two methods therefore complement each other and together provide a comprehensive picture of population history.

Fig trees are keystone biological resources in tropical and subtropical habitats worldwide (Cook & Rasplus 2003; Harrison 2005), and fig fruits and their insect inhabitants are important model systems in the study of community assembly and coevolution (Cook & Rasplus 2003; Segar et al., 2014). Our target species *Pleistodontes nigriventris* is the specialist pollinating wasp of *Ficus watkinsiana* (Lopez-Vaamonde et al., 2002; Male & Roberts 2005, Rønsted et al., 2008), a rainforest fig restricted to northern and southern populations over 1000km apart along the eastern coast of Australia (Fig. 2) (Dixon 2003). The distribution of Australian rainforests has been dictated by two major processes. First, falling temperatures during the Miocene restricted them to areas of higher rainfall along the eastern and southern coasts (Markgraf et al., 1995), separated from drier inland habitats by the Great Dividing Range (Chapple et al., 2011) (Fig. 2). Second, during the Pleistocene climate oscillations, east coast Australian rain forests repeatedly expanded from, and contracted into, a latitudinal series of refugia separated by intervening areas of dry forest and shrublands (Bryant & Krosch, 2016; Chapple et al., 2011). The rainforest areas occupied by *F. watkinsiana* are currently separated by two major dryland corridors (Fig. 2): the Burdekin Gap, located between Mackay and Townsville, is the largest dry land corridor on the east coast, and the St. Lawrence Gap is a smaller lowland dry corridor located 350km further south (Weber et al., 2014; Bryant & Krosch, 2016). While the formation and stability of these dryland corridors through

time is incompletely characterised (Bryant & Krosch, 2016), both have been implicated in restricting dispersal and driving population divergence in rainforest plants (Burke et al., 2013), including *F. watkinsiana* (Dixon, 2003H; Haine & Cook, 2005) and animals (e.g. Schauble & Moritz, 2001; Pope et al., 2001; Nicholls & Austin, 2005; Brown et al., 2006; Dolman & Moritz, 2006; Baker et al., 2008, MacQueen et al., 2012; Rix & Harvey, 2012; Bryant & Fuller, 2014; Bryant & Krosch, 2016).

The impact of biogeographic barriers on the genetic makeup of any species depends on how long ago population divergence occurred, the sizes of the populations, and the direction, mode and frequency of gene flow between them (Aeschbacher et al., 2017; Ringbauer et al., 2018). Previous studies of fig/fig wasp systems provide evidence for two contrasting paradigms with which patterns in *Pleistodontes nigriventris* can be compared. Female fig wasps are poor active flyers (and the males are wingless and do not leave their natal fig) (Ware & Compton 1994a,b), and we might therefore expect limited dispersal, restricted gene flow and substantial population structure in geographically widespread species. This hypothesis is supported by the observation that some widespread fig species are pollinated by a geographically structured suite of distinct fig wasp taxa (Chen et al., 2012; Wachi et al., 2016; Rodriguez et al., 2017; Yu et al., 2019). This paradigm predicts high genetic divergence between northern and southern populations of *P. nigriventris*. However, some fig wasps are dispersed over large distances by wind currents above the tree canopies (Ahmed et al., 2009; Liu et al., 2015), particularly when emerging from fig fruits high in the forest canopy (Harrison & Rasplus, 2006; Kobmoo et al., 2010; Yang et al., 2015; Liu et al., 2015; Sutton et al., 2016). Two studies of such systems have found little genetic differentiation in pollinating fig wasps over distances ranging from several hundred to >1500 km (Kobmoo et al., 2010; Liu et al., 2015; Bain et al., 2016). *Ficus watkinsiana* can grow to 50m, and if *Pleistodontes nigriventris* benefits from wind-assisted dispersal, we might expect to find significant gene flow between *F. watkinsiana* populations. Here we answer the following questions for *Pleistodontes nigriventris*:

1) Is there evidence of genetic divergence between populations either side of the Burdekin and St. Lawrence Gaps?

2) Is there a signal of post-divergence gene flow, and if so, in which direction?

3) Can we discriminate between the IM and ADM models of gene flow?

4) Do the blockwise and PSMC methods infer concordant population histories?

5) Is the inferred divergence time for *P. nigriventris* concordant with estimates for other co-distributed taxa?

Materials and Methods

Sample Collection

Samples were collected between January 2001 and August 2009 from four sites in Queensland, two in each of the northern and southern ranges of *F. watkinsiana.* The two Northern individuals were sampled from Kairi (N1: 17.21° S, 145.55° E) and Kamerunga (N2: 16.87° S, 145.68° E) and the two South individuals were sampled from Settlers Rise (S1: 27.68° S, 153.26° E) and Main Range (S2: 28.07° S, 152.41° E) (Fig. 2). Near-to-ripe *F. watkinsiana* fruits were collected and placed individually into specimen pots. Our sampling targeted male fig wasps, whose haploid genome facilitates analysis (Bunnefeld et al., 2018; Hearn et al., 2014). Once the wasps started to emerge (12-24 hours after collection depending on fig ripeness) figs were dissected and live males were placed directly into 70% ethanol to preserve for DNA extraction. Due to potentially high levels of sib-mating in fig wasps (Greeff et al., 2009; Sutton et al., 2016) all individuals were sampled from different figs.

DNA extraction and sequenced-based confirmation of identity.

DNA was extracted from whole male wasps 1.5-1.6mm long (Lopez-Vaamonde et al., 2002) using the Qiagen DNeasy Blood and Tissue Extraction kit. The Purification of Total DNA from Animal Tissues (Spin-Column) Protocol was followed with the following modifications to maximise DNA yield from these extremely small wasps. Step 1: Individual wasps were placed in 180 µl of buffer ATL and crushed using a mini-pestle. Step 2: Riboshredder RNase (Epicentre) was used in place of RNase A. Steps 7-8: Buffer EB was used in place of Buffer AE for the elutions as Buffer AE contains EDTA, which will interfere with the downstream library preparation. Extractions

were eluted in smaller volumes (25 µl) than recommended and samples were incubated for longer (5 minutes). This protocol yielded 35.7-58.3 ng of DNA per wasp, despite their very small size (total body length *ca.* 1mm).

Identification of male fig wasps was confirmed by comparison of sample sequences to voucher sequences for a 433 base pair (bp) fragment of the mitochondrial cytochrome b (cytb) gene (Lopez-Vaamonde et al., 2001). Sequences were amplified using the primers CB1/CB2 (Jermiin & Crozier, 1994). 0.3 µl of DNA extraction was used per PCR reaction. The remainder of the PCR mix consisted of 2 µl BSA (10 mg/ml), 2 µl 10X PCR buffer, 0.8 µl MgCl2 (50mM), 0.3 µl of each primer (20 µM), 0.16 µl dNTPs (each 25 mM) and 0.1 µl Taq (Bioline 5U/µl), made up to 20 µl with autoclaved MilliQ water. Amplification was carried out using a Bio-Rad S1000 thermal cycler for 2 minutes at 94°C, 35 cycles of 30 seconds at 94°C, 30 seconds at 48°C, 40 seconds at 72°C, and a final elongation step of 5 minutes at 72°C. PCR products were visualised on a 2% agarose gel and cleaned using a shrimp alkaline phosphatase and exonuclease 1 protocol. 2.5 µl of SAPExo1 mix (1.425 µl SAP dilution buffer, 1 µl SAP (1U), 0.075 µl Exo1 (1.5U)) was added to each sample before being incubated for 40 minutes at 37°C followed by 15 minutes at 94°C. Only the forward strand was sequenced for each individual, using BigDye chemistry on an ABI 3730 machine at the Edinburgh Genomics facility. Sequences for the four individuals have been deposited on GenBank (individual accession numbers: N1 MF597824; N2 MF597800; S1 MF597825; S2 MF597826).

High-throughput library preparation and sequencing

We generated an Illumina Nextera genomic library for each individual male fig wasp following the manufacturers' instructions. To make best use of paired end sequencing, the library fragment size distribution should be unimodal with a majority of fragments longer than the 150bp read length. We checked the fragment size distribution by running 1µl of each library on a high sensitivity DNA Bioanalyzer chip (Agilent 2100). Libraries for each individual were end-labelled using a unique pair of indices, pooled and sequenced in one lane of 150bp paired-end reads on the Illumina HiSeq platform at the Edinburgh Genomics facility. Pooling volumes were calculated to

achieve ~6-fold coverage per individual assuming 50 gigabases of data per lane and a genome size of 300 Mb based on an estimate for another Agaonid fig wasp, *Ceratosolen solmsi* (278 Mb; Xiao et al., 2013). The short read data have been deposited at the ENA short read archive (Cooper et al., 2020a).

Bioinformatic pipeline

Reads for all four individuals were screened to remove low quality and contaminant reads and combined. After exclusion of contaminants, reads for all four individuals were combined to generate a *de novo* meta-assembly for *P. nigriventris* using *SPAdes* (version 3.6.2) (Bankevich et al., 2012). Reads from each individual were mapped back to this reference using BWA; variants were called using *GATK* haplotype caller. After masking repeat sequences, sites with a minimum coverage of two and a mapping quality (>20) and base quality (>10) were identified using the *GATK* tool *CallableLoci*. The bioinformatic pipeline is summarised diagrammatically in Supplementary information, Figure S1.

(i) *Quality control and processing of sequencing reads*. To exclude low quality sequence, reads were checked using *Fast-QC* (www.bioinformatics.babraham.ac.uk/projects/fastqc) and trimmed at a base quality score of 20 (sliding window 15:20 and min length 50). Adapters were trimmed using *Trimmomatic* version 0.32 (Bolgar et al., 2014). Any adaptors found to be present after a second pass through *Fast-QC* were removed using *Cutadapt* (Martin, 2011). Paired-end reads were merged using *PEAR* version 0.9.0 (Zhang et al., 2014) for *de novo* assembly only.

(ii) *Filtering of contaminant sequences*. Genomic data obtained from whole organism libraries commonly contain reads from associated non-target organisms, including symbionts, parasites and commensals. *Wolbachia* bacteria are common endosymbionts in fig wasps (Haine and Cook, 2005) and diverse fungal taxa have been identified from a genome assembly of the fig wasp *Ceratosolen solmsi* (Niu et al., 2015). To remove contaminant sequences from our data, we first aligned reads across all 4 individuals to a *Velvet* assembly (version 1.2.10) with a k-mer length of 31 (Zerbino and Birney, 2008). The filtered reads for each individual were mapped to an initial *Velvet* reference assembly using *Bowtie2* version 2.2.3 (Langmead and Salzberg, 2012).

Contaminant sequences were identified using blobtools (Kumar et al., 2013), which uses BLAST searches to create Taxon-Annotated-GC-Coverage plots (Blobplots) that allocate aligned reads to taxa at a user-specified level. We used four BLAST approaches to assess taxonomic matches: (i) The fast protein aligner *Diamond* (version 0.7.9) (Buchfink et al., 2015) was used alongside three BLAST (version 2.2.29) searches: (ii) against the NCBI nucleotide database (https://www.ncbi.nlm.nih.gov/nucleotide/), (iii) against the genome of the Agaonid pollinating fig wasp, *Ceratosolen solmsi* (Xiao et al., 2013), and (iv) against the genome of the pteromalid parasitoid wasp *Nasonia vitripennis* (Werren et al., 2010). Non-Arthropod reads (primarily allocated to Proteobacteria and Ascomycota) were excluded from further analysis.

(iii) *Generation of a P. nigriventris reference assembly*. After exclusion of contaminants, reads for all four individuals were combined and re-assembled using *SPAdes* (version 3.6.2) (Bankevich et al., 2012). The quality of this reference assembly was assessed using *BUSCO* (*Benchmarking Universal Single-Copy Orthologs*) version 1.1b1 (Simão et al., 2015) using the Arthropoda *BUSCO* set (http://busco.ezlab.org).

(iv) *Variant calling*. Filtered, merged reads from each individual were mapped back to the reference meta-assembly using the *Burrows-Wheeler Aligner* (*BWA)* version 0.7.10 (Li & Durbin, 2009). FASTA file indexes and sequence dictionaries were created using *samtools* (Li et al., 2009) *faidx* (version 1.2) and the *picard* (https://broadinstitute.github.io/picard/index.html) tool *CreateSequenceDictionary* (version 1.141) respectively. The BAM files were sorted and merged to create a single species BAM file using the *picard* tool *MergeSamFiles*. Duplicate reads were removed from these merged files using the *picard* tool *MarkDuplicates*. Variants were called using *HaplotypeCaller* in *GATK*. As male wasps are haploid, ploidy was set to 1 and the '-emit variants only' option was used. Only SNPs were considered.

(v) *Masking repetitive regions*. Regions of repetitive DNA can cause assembly and mapping errors in short read data (Treangen & Salzberg, 2011). We created a library of repetitive regions in the reference meta-assembly using *RepeatScout* (version 1.0.5) (Price et al., 2005), and masked these using *RepeatMasker* (version open-4.0.6) (Smit, AFA, Hubley, R & Green, P. *RepeatMasker*

Open-4.0. 2013-2015 http://www.repeatmasker.org). *RepeatMasker* outputs an annotation file which was used to create a BED file of repeat positions for downstream processing.

(vi) *VCF filtering*. High quality sites were identified based on coverage and mapping quality using the *GATK* tool *CallableLoci* and default parameter values except for the following: minimum base quality of 10, minimum mapping quality of 20, minimum read depth of two reads per site. The base quality score recalibrated (BQSR) BAM file was subsampled to extract BAM files for each individual. We used *CallableLoci* to generate BED files of callable regions in each individual. Repeat regions were excluded and positions meeting filters across all four individuals extracted using *bedtools multiIntersectBed*. This BED file was used to filter the VCF files (generated from the *GATK* pipeline) for callable variable sites using *bcftools* (Li, 2011) version 1.2.

Fitting of IM and ADM models

(i) *Specification of alternative IM and ADM divergence models*: Both the IM and the ADM model assume an ancestral population with a constant effective population size (N_a) that splits into two populations (North and South). One of the descendant populations maintains the same ancestral population size N_a, whilst the other is free to change to (*1/B)* x N_a (i.e. *B* scales the rate of coalescence in the other population). In both models (Fig. 1), population divergence occurs at time *T* in the past. In the IM model divergence is followed by continuous unidirectional migration at rate *M = 4Nm* migrants per generation (m is the per lineage probability of migrating). In the ADM model (Fig. 1), gene flow occurs through an instantaneous and unidirectional admixture event at time T_{adm} which transfers a fraction *f* of lineages from the donor population into the recipient (Fig. 1). All time parameters are scaled in $2N_a$ generations. We assessed support for all four possible combinations of population size and gene flow under both the IM and ADM models (Figure S2), as well as for simpler nested models which either involving gene flow but a single population size parameter (B=1) or two population sizes but no post-divergence gene flow.

(i) *Generation of blockwise site frequency spectra (bSFS)*: We used the composite likelihood calculation described in Lohse et al. (2016) to fit the IM and ADM models (see also Jordan et al., 2017 and Nürnberger et al., 2017). The method uses information in patterns of linked sequence

variation contained in short blocks and has previously been used for demographic inference under a variety of demographic scenarios including the IM model (Lohse et al., 2012) and models of discrete admixture (Bunnefeld et al., 2018). For a sample of four haploid individuals (two from each of the North and South populations), we can distinguish four mutation types: variants in the two Northern samples (Nvar), variants in the two Southern samples (Svar), fixed differences between North and South (Fixed differences), or variants shared between North and South (Sharedvar) (Lohse et al., 2016). The site frequency spectrum of a block (bSFS) consists of counts of these four site types, i.e. vector {Nvar, Svar, Sharedvar, Fixed}. We used the automated recursion implemented by Lohse et al. (2016) to obtain the generating function of genealogies under the ADM model and computed the composite likelihood of both the ADM and IM models in *Mathematica* as described in Lohse et al. (2016) and Nürnberger et al. (2017).

The likelihood calculation assumes an infinite sites mutation model and no within-block recombination. Given these assumptions, blocks that contain both fixed difference and shared variants (violating the 4-gamete test) are not possible and were excluded from the likelihood calculation. We chose a block length that strikes a balance between potential bias (arising from recombination within blocks) and power (which suffers when too few blocks contain multiple variant sites). We used a custom python script to extract aligned sequence blocks of a fixed length of 387 base pairs, which corresponds to an average of 1.5 variant sites per block. The blockwise data were analysed in *Mathematica* (Wolfram Research, Inc., Mathematica, Version 10.4, Champaign, IL (2016)) (Cooper et al., 2020b). The computational cost of calculating composite likelihoods increases with the number of unique bSFS configurations considered in the data. We limited the number of bSFS configurations by lumping mutation counts above a threshold k_{max}= 2 for the Nvar, Svar and SharedVar and k_{max}= 3 for fixed differences. Since 87% of the blockwise data are within these k_{max} bounds and so included in the composite likelihood calculation exactly, the expected loss of power is minimal.

(iii) *Estimation of demographic parameters*: We estimated all model parameters for both the IM and ADM model. Estimation of N_a *(as* N_a *= theta /(4* μ*))* and scaling of *T* parameters into years requires an estimate of the mutation rate per generation (μ) and the number of fig wasp generations (*g*) per

year. In the absence of any fig wasp estimate of μ, we used the per generation mutation rate of 2.8 x 10^{-9} for *Drosophila melanogaster* (Keightley et al., 2014). Note that the relative timing of events in different models is not affected by this calibration. We assumed four fig wasp generations per year ($g=4$) and converted time estimates into years by multiplying by $2N_a$ and dividing by g.

(iv) *Correcting for the effects of linkage between blocks.* The composite likelihood calculations do not account for linkage between blocks. Given the difficulty of assessing the level of linkage between blocks in highly fragmented assemblies, we incorporated linkage effects using a parametric bootstrap approach (Lohse et al., 2016). We used *msprime* (version 0.3.1 (IM) and 0.4.0 (ADM)) (Kelleher et al., 2016) to simulate 100 datasets assuming a recombination rate of 2.719 x 10^{-10} per base (estimated from the data, see below). Each dataset consisted of 20 continuous stretches of recombining sequence and had a total length matching the real data. Fitting the inferred model to these simulated datasets, we obtained 95% confidence intervals for parameter estimates as ±1.96 standard deviations (of the analogous estimates on the simulated data).

(v) *Model selection*. We used an analogous parametric bootstrap scheme to determine whether the IM or ADM models provided a significantly better fit to our data. We fitted both models to each of 100 bootstrap datasets simulated under the best-fit IM model parameters. The distribution of differences in log composite likelihood (calculated as ΔlnCL = 2*(ADMlnCL-IMlnCL)) between the IM model and the ADM model represents an expectation of selecting the ADM when the IM is true (Type 1 error). We determined critical values from this distribution at a significance level of 0.05.

(vi) *Recombination rate estimation*. There are no estimates of either the per generation recombination rate (r) or the population recombination rate ($\rho = 4Ner$) for any fig wasp species. We therefore estimated a recombination rate for *P. nigriventris* using a two-locus generating function that co-estimates ρ (scaled by $2Ne$) and θ, for a sample of two haploid genomes drawn from a single panmictic population (here, the two Northern individuals) (Lohse et al., 2011).

PSMC analysis

We compared the results of our blockwise analysis with inference using the Pairwise Sequentially Markovian Coalescent (PSMC) (Li & Durbin, 2011). PSMC infers the effective population size history of a single diploid individual, and can also be applied to a pair of haploid genomes. PSMC provides a continuous estimate of demographic parameters through time. While PSMC does not allow to infer population divergence directly, comparison the PSMC trajectories of two diverged populations (here, North and South) reveals when these shared the same population size and so were likely part of the same ancestral population.

PSMC uses the density of pairwise differences along the genome to infer a trajectory of population size through time. Input files were generated from the per-individual BAM files using *samtools mpileup* (version 0.1.19). The pileup file was converted to a VCF file in *bcftools* (version 0.1.19) and a consensus sequence (fastq file) per individual was generated using the *bcftools* utility *vcf2fq*. Consensus files contained 31,371 and 33,523 contigs for the North and South pairs respectively. The two consensus files per population were merged using the *seqtk* function *mergefa* (version 1.0) and converted to the PSMC input format using the PSMC function *fq2psmcfa* (version 0.6.5). Only contigs that contain >10kb of unfiltered bases, ≥ 80% of which pass a quality threshold score, here set to ≥20 were included (6,900 and 7,305 contigs for the North and South pairs respectively). We analysed each pair of individuals with PSMC (version 0.6.5) using the following parameter values: N = 30, t = 20, r = 10.3 and p = “4+60*1+4”. Each dataset was sub-sampled 100 times to generate bootstrap replicates using the PSMC utility *splitfa* (version 0.6.5). Results were calibrated using the same mutation rate and generation times given above.

Results

De novo genome assembly for *Pleistodontes nigriventris*

Nextera libraries were generated successfully for all four male *Pleistodontes nigriventris* (Figure S3). After initial filtering and trimming the joint assembly of reads for all four individuals in

Velvet contained 173,180 contigs ≥200bp (Table S1). We identified contaminant reads from a range of non-Arthropod taxa (Figure S4). Individual assemblies contained between 5k and 149k reads identified as bacterial. For three individuals over 97% of these were attributed to *Wolbachia* (and 24% in the final individual) (Table S2). The relative fraction of *Wolbachia* reads was significantly higher in Northern compared to Southern individuals (Chi-squared = 95159, df = 1, p < 2.2e-16), consistent with previous findings of between-population differences in *Wolbachia* prevalence in *P. nigriventris* (Haine & Cook, 2005). Excluding contaminant reads resulted in between 11 and 22.5 million reads per individual (Table S1). Re-assembly using *SPAdes* improved the contiguity (139,731 contigs ≥200bp, N50 of 9,643 bp) and the completeness of the final assembly: CEGMA scores: 93.15% complete and 99.19% partially complete, *BUSCO* scores for the reference Arthropod gene set: 74% complete, 4.5% duplicated, 16% fragmented and 8.4% missing . We note that the *P. nigriventris* assembly, although fragmented, has higher completeness (in terms of complete Core Eukaryote Genes) than the genome of *Ceratosolen solmsi* (CEGMA: 88% complete), the only published fig wasp genome (Xiao et al., 2013). Repetitive elements made up 21.4% of the reference assembly and were excluded from subsequent analyses.

Processing of the filtered and aligned reads (mean coverage per individual of 3.7x) identified 1,837,396 SNPs. The average pairwise diversity per site (after filtering) for the North and South populations were very similar (π = 0.000884 and 0.000822 respectively). This is one of the lowest estimate of genetic diversity reported for any sexually reproducing arthropod (Leffler et al., 2012; Romiguier et al., 2014). Pairwise *Fst* was 0.74, indicating high differentiation between the Northern and Southern populations.

Inferring divergence with continuous migration and admixture

Our block extraction protocol resulted in 775,977 blocks of 387 base pairs (Cooper et al., 2020b). Of these, 0.8% (5,872) contained both shared variants and fixed difference, violating the 4-gamete test, and were excluded from blockwise analyses.

374 *Isolation with continuous migration (IM).* Models incorporating post-divergence migration and different effective population sizes (N_e) received substantially greater support than otherwise
376 equivalent models with no migration and/or a single N_e parameter (Table 1a). The best-supported direction of migration is from South to North, irrespective of whether we assumed a single N_e
378 (compare model IM3 to IM2) or two N_e parameters (compare IM7+IM9 to models IM6+IM8). The scenario in which the Southern population retained the ancestral N_e (IM9; Figure S2) had highest
380 support. Under this model, the split between the two populations occurred 177 (95% C.I. 172–182) thousand years ago (kya) and the N_e for the ancestral/Southern population was estimated to be
382 slightly higher (69k, 95% C.I. 65.4k-72.6k) than for the Northern population (58k 95% C.I. 54.3k-61.5k). We inferred a migration rate *M* from South to North of 0.071. Although low (1 migrant from
384 South to North every 28 generations), this estimate was significantly greater than zero (95% C.I. 0.045 – 0.097).

386 *Isolation with instantaneous admixture (ADM)*. Inferences for models assuming instantaneous admixture mirrored those for IM models both in terms of model comparisons and parameter
388 estimates: scenarios with gene flow and two N_e parameters were significantly better supported than otherwise equivalent models without admixture and/or a single N_e (Table 1b). The best-
390 supported admixture direction was again from South to North, and the model assuming that the Southern population retained the ancestral N_e (ADM10; Figure S2) had greatest support. N_e
392 estimates under the best fitting ADM history were similar to those under the analogous IM model (IM9): we inferred an ancestral/Southern N_e of 69k (95% C.I. 66.1k-72.6k) and a lower Northern N_e
394 of 59k (55.2k-62.2k). In contrast, under the best fitting ADM9 the population split was estimated 196kya (95% C.I. 193-198kya), slightly older than under the analogous IM model. The admixture
396 event was inferred to have occurred 57kya (95% C.I. 53-62kya) (Table 1b) and around a quarter (admixture fraction f = 0.239, 95% C.I. 0.206-0.272) of Northern lineages are inferred to have
398 originated from the Southern population.

Greater support of instantaneous admixture. The ADM model had greater support than the IM
400 model (ΔlnCL = 4175). Since the blockwise composite likelihood calculation ignores linkage between blocks and given that IM and ADM models are not nested, we cannot use a likelihood

ratio test to compare the support for these models. To confirm whether the simpler IM model fits significantly worse than the ADM model we obtained a critical value for ΔlnCL (155.4 at p=0.05) using a fully parametric bootstrap. The difference in model support in favour of the ADM model ΔlnCL = 4175 in the real data far exceeds this and confirms that admixture provides a better fit to our data than continuous gene flow. To investigate which aspect of blockwise variation in the data allows discrimination between instantaneous admixture (ADM) and continuous migration (IM), we compared the frequencies of the most common bSFS configurations in the data with those expected under the best fitting IM and ADM models (Figure S6). Inspection of the residual reveals that the ADM model predicts both the frequency of monomorphic blocks ({0,0,0,0}) and blocks with more than three fixed differences ({0,0,>3,0}) better than the IM model.

PSMC supports divergence and instantaneous admixture from South to North

We used PSMC (Li & Durbin 2011) to infer trajectories of population size change for Northern and Southern populations. Comparing the trajectories both with each other and with parameters inferred under the best fitting models of divergence and gene flow (ADM10) reveals a close correspondence between blockwise analyses and PSMC in several respects (Fig. 4). First, PSMC trajectories are consistent with the blockwise inference of a slightly larger N_e in the Southern population compared to the North. Second, the divergence time inferred by the blockwise analyses corresponds to a period in the PSMC at which the Northern and Southern populations show similar N_e (overlapping confidence intervals), consistent with a shared ancestral population. Finally, PSMC infers an increase in the Northern N_e prior to the time of admixture inferred under the ADM model. Such an increase in genetic diversity in the (Northern) recipient population is exactly what would be expected from a sudden admixture event. We note that PSMC also reveals an increase in the Southern N_e around the same time which, however, is markedly smaller. While PSMC also shows an increase in N_e in the very recent past (i.e. the last 3ky), the variation among bootstrap replicates (Fig. 5) suggests that our data lack the signal to reliably infer population size change over this timescale.

Discussion

Individual level population genomics of very small insects

We generated genomic libraries for individual male fig wasps, each only 1.5 mm long, resulting in over 770 thousand aligned blocks of sequence containing an average of 1.5 variable sites. Even with minimal samples of two haploid individuals per population, whole genome data allows estimation of demographic parameters with high confidence. The best supported IM and ADM models gave similar estimates for the age of the initial divergence between Northern and Southern *P. nigriventris* populations, and their sizes. Further, we show that a burst of admixture (ADM) provides a significantly better fit than ongoing gene flow to the blockwise data and the individual population N_e trajectories inferred by PSMC analysis. We first place our results in the broader context of phylogeographic work on taxa spanning the Burdekin and St. Lawrence Gaps, and then discuss the potential limits of our demographic inferences.

Pleistocene population divergence and gene flow across the Burdekin and St Lawrence Gaps in *P. nigriventris*

Australia has a complex climate history, a major feature of which is the aridification that started in the Miocene and continued throughout the Pliocene and Pleistocene (Schauble & Moritz, 2001; Martin, 2006; MacQueen et al., 2010, Frankham et al., 2016). This resulted in the gradual restriction of rain forests to the Eastern coast of Australia, separated from more arid inland habitats by the Great Dividing Range (Kershaw 1994; McGuigan et al., 1998; Schneider et al., 1998; Pope et al., 2000, Bell et al., 2007). Between 280 and 205kya, decreased precipitation and more severe aridification were associated with major faunal turnover in rainforest taxa (Hocknull et al., 2007). Against the backdrop of this general trend, the Pleistocene climate oscillations drove cycles of rain forest expansion during warmer, wetter interglacials and contraction during cooler, drier glacials (Byrne 2008; Maldonado et al., 2012; Burke et al., 2013). The current dry habitat corridors of the Burdekin and St. Lawrence Gaps are thought to be products of the long term aridification of

Australia, and though it is uncertain when they first formed, they most likely existed through multiple Pleistocene cycles (Bryant & Krosch, 2016).

We found a strong signature of population divergence over the combined Burdekin and St. Lawrence gaps in *Pleistodontes nigriventris*. This is perhaps to be expected, given the obligate dependence of *P. nigriventris* on *Ficus watkinsiana,* and the restriction of this fig species to rain forest (Dixon 2003). However, our analyses do not allow inference of the ancestral distribution of *P. nigriventris,* and are compatible with either population being founded from the other, or vicariance of a previously continuous rainforest distribution (Martin, 2006). The best fitting IM and ADM models for *P. nigriventris* agree that the divergence between the Northern and Southern populations occurred 170-200kya ago, in the Late Pleistocene.

In a review encompassing a wide range of plant and animal taxa, Bryant and Krosch (2016) identified a signature of population subdivision for the Burdekin Gap in 18 of 27 studies (nine of which have divergence time estimates) and for the St. Lawrence Gap in 10 of 23 studies (six of which have divergence time estimates). Pleistocene divergence across the Burdekin Gap has also been inferred for *Melomys cervinipes* (a wet forest rodent (Bryant & Fuller (2014)), *Petaurus australis* (yellow-bellied glider (Brown et al., 2006)), and *Varanus varius* (a large lizard with broad habitat preferences (Smissen et al., (2013)). Very few studies have considered insect population structure across the same potential barriers to gene flow. In contrast to our results for *P. nigriventris,* Schiffer et al., (2007) found no evidence for genetic divergence across the Burdekin gap in *Drosophila birchii*, a specialist rainforest fruit fly, but instead inferred a moderate gene flow across the whole range following a recent range expansion. Divergence estimates for other taxa spanning the Burdekin and/or St Lawrence Gaps are concentrated in the late Miocene to late Pleistocene (Bryant & Krosch 2016) with substantial variation across taxa. For example, divergence across the Burdekin Gap was estimated to have occurred in the early Miocene-late Oligocene >20 million years ago (mya) in *Uperoleia* frogs (Catullo & Keogh 2014; Catullo et al., 2014), and 31-51mya in assassin spiders (Rix & Harvey 2012). Given that most of these previous estimates are not based on any statistical model of population divergence, but rather a single (often mitochondrial) gene tree, it is unclear how much of the variation in previous divergence time

482 estimates across these co-distributed taxa simply reflects coalescence variance and/or differences in calibration. Model based comparative studies are needed to assess whether past vicariance
484 events have been shared in time across taxa with disjunct distribution across the Burdekin and St Lawrence gap.

486 The Northern population of *P. nigriventris* received a burst of admixture from the South at the end of the Pleistocene

488

Both the best fitting ADM and IM models inferred gene flow from the Southern to the
490 Northern population. While the continuous migration rate inferred under the best IM model (*M* = 0.071) is much lower than the estimated admixture fraction (f=0.24) under the better supported
492 ADM model, the overall amount of gene flow inferred under both models is in fact very similar: Under the IM model, the probability that a single lineage sampled from the North is derived from
494 the South via gene flow is 1-e^(-*MT*). Given our estimates for these parameters in model IM9, this is ~0.3, so very comparable to the admixture fraction inferred under the best ADM model. While
496 both models agree in the overall amount of post-divergence gene flow, our model comparison clearly shows that genetic exchange occurred as a sudden burst rather than a continuous process.
498 Additional support for a discrete admixture event comes from the contemporary increase in the Northern population size revealed by PSMC. The inferred combination of divergence and
500 admixture is compatible with the following demographic scenario: (i) Northern and Southern populations were separated 170-200 kya following contraction of suitable habitat and expansion of
502 intervening inhospitable dry forest corridors. (ii) Northern and Southern populations remained separated for over 100ky until favourable conditions in the late Pleistocene allowed expansion of
504 one or both populations of *Ficus watkinsiana,* to the point at which substantial genetic exchange was possible between populations of pollinating *P. nigriventris*. (iii) Subsequent aridification
506 resulted again in range contractions and a shutdown of gene flow.

Notwithstanding the uncertainty in our time calibration for *P. nigriventris,* the date of the
508 inferred admixture event falls in Marine Isotope Stage 3 (27-60kya), a period in the late Pleistocene

characterised globally by abrupt phases of warming and cooling (Siddall et al., 2008; Van Meerbeeck et al., 2009). These warming phases were interspersed by cooler periods around every 7,000 years (Clark et al., 2007), and even during the cooler periods average temperatures were much higher than during the Last Glacial Maximum (~19-21kya) (Van Meerbeeck et al., 2009). The lower bound (53kya) of the inferred admixture time corresponds approximately to the warmest point in one of these cycles, and it is tempting to suggest that this allowed temporary expansion of the range of the *F. watkinsiana*/*P. nigriventris* mutualism and secondary genetic contact.

Our results do not rule out bidirectional dispersal, but rather imply a signal of predominant gene flow from the South into the North. This could indicate conditions that facilitated northwards dispersal in this direction, such as prevailing winds from the south. Records from the 1940s-2000s do indicate stronger winds from the south in eastern Australia (Australian Government, Bureau of Meteorology, http://www.bom.gov.au/climate/). However, it is not known whether current trends can be extended back into the past. Similar post-divergence dispersal from south to north across the Burdekin gap has been inferred in a small number of other rain forest-associated taxa (Bryant & Fuller, 2014; Bryant & Krosch 2016). Alternatively, the asymmetry in genetic exchange between North and South we infer may be the result of genetic incompatibilities that arose and became fixed during periods of isolation.

Limits of demographic inference

Demographic analyses that are based on genome-wide samples of either single variants or loci/blocks generally assume that blocks are statistically independent. A common way of dealing with linkage effects is to use subsampling, either by sampling a fixed minimum distance apart or by resampling bootstrap. We have instead opted for a fully parametric bootstrap that incorporates linkage between blocks explicitly. Although this is computationally more intensive than subsampling, we believe it is the only way to accurately capture the effect on parameter estimates. Our parametric bootstrap for the best fitting IM and ADM models gave narrow 95% confidence intervals for all model parameters. Importantly, mean parameter estimates obtained from the simulation replicates are very close to the MLEs used to simulate the datasets (Table 1). This

536 confirms that biases in parameter estimates due to violations of the assumption of no recombination within blocks are negligible, as shown in previous studies on a range of organisms 538 (Jennings & Edwards, 2005; Lanier & Knowles, 2012; Hearn et al., 2014; Bunnefeld et al., 2015; Wang & Liu, 2016). Another standard assumption of demographic inference is that sequences 540 evolve neutrally. While our approach sampled blockwise sequence variation genome-wide, one would expect both genome assembly and read mapping to be easier in regions under selective 542 constraint. As a consequence, our blockwise dataset is likely enriched for conserved coding regions. In a methodologically similar study of a European gall wasp, Hearn et al., (2014) tested for 544 the effect of selective constraint by partitioning blocks according to the proportion of coding sequence they contained, and scaling the estimated genome-wide mutation rate between values 546 for synonymous and non-synonymous mutations. They found that mutation rate heterogeneity had no impact on the inference, reporting only a slight increase in N_e and divergence time estimates. 548 Given these results and the lack of annotated genomes or transcriptome data to aid gene detection, we have not pursued this here. However, it will be interesting to check whether selective 550 constraint can explain the observed higher frequency of invariant blocks in our *P. nigriventris* data compared to expectations under both the best fitting IM and ADM models. Taken together, these 552 results suggest that recombination within blocks and background selection had a minimal impact on our inference of demographic history.

554 Scaling divergence and admixture times into years requires knowledge of both the mutation rate and generation time. Both are uncertain for *P. nigriventris.* In the absence of direct mutation 556 rate estimates for fig wasps, we used an estimate from *Drosophila melanogaster* (Keightley et al., 2014). While it is unclear how well this matches mutation rates in fig wasps, it is reassuring that the 558 few published mutation rate estimates for other insects are similar (e.g. 2.9×10^{-9} for the butterfly *Heliconius melpomene*). A likely greater source of calibration uncertainty is the generation time, 560 which is unknown for *P. nigriventris* and fig wasps in general. Liu et al. (2014) give 2-3 generations per year for the *Wiebesia* sp. fig wasp pollinator of a dioecious fig in eastern China, but we are 562 unaware of any estimates for pollinating wasps associated with monoecious fig species. The lack of precise generation time information is due primarily to the fact that, like many tropical

564 monoecious figs, *F. watkinsiana* fruits asynchronously year round (Harrison, 2005), with no clear seasonal cycle to entrain pollinator generations. Based on personal observation (JMC and Tim
566 Sutton, Western Sydney University), a range of 2-6 generations per year seems likely. Assuming 2 and 6 generations per year (rather than 4 as we have done here) would still place divergence and
568 admixture times for *P. nigriventris* in the late Pleistocene. However, in the absence of precise information our attempt to match the demographic history of *P. nigriventris* to past climatic events
570 remains speculative.

572 All three demographic scenarios we have considered (IM, ADM and PSMC) are obviously crude simplifications of what is likely a more complex history possibly involving repeated cycles of rain
574 forest expansion and contraction. The upland wet forests south of the Burdekin Gap in the Clarke Range and Conway Peninsula are thought to have persisted through multiple Pleistocene climate
576 cycles (Stuart-Fox et al., 2001), and it would be interesting in future to explore more realistic histories involving repeated admixture (Jésus et al., 2006) in *P. nigriventris* and *F. watkinsiana*.
578 However, the fact that our parameter estimates are consistent across models and the close fit of the ADM model to the blockwise data in absolute terms, suggest that we have captured key
580 aspects of the demographic history of *P. nigriventris.* It is also encouraging that, as we have shown, continuous and discrete gene flow can be clearly distinguished in this species, even over
582 relatively recent timescales (both in terms of sequence divergence and genetic drift).

Our results show that robust demographic inferences can be made for very small sample sizes of
584 non-model taxa without significant associated genomic resources. Such approaches are likely to be increasingly useful for taxa that are rare or hard to sample. Figs support highly structured (and
586 often co-evolved) communities of pollinators, inquilines and natural enemies (Lopez-Vaamonde et al., 2001; Segar et al., 2014), and while a growing body of work addresses phylogeographic
588 relationships in figs and their pollinators (Bain et al., 2016; Rodriguez et al., 2017; Yu et al., 2019), much less is known about the phylogeography of non-pollinating fig wasps (Sutton et al., 2016).
590 Our approach provides a framework for comparative analyses that reconstruct the assembly of these species-rich communities. More broadly, given that many questions about both intraspecific

592 demography history and speciation come down to distinguishing between ongoing gene flow and discrete admixture pulses, systematic power analyses on how this can best be achieved - 594 especially for genomic data from non-model organisms without a contiguous reference genome - are urgently needed.

596 Acknowledgements

This work was funded by a UK NERC grant (NE/J010499) to GS, KL and JMC. LC was supported 598 by a PhD studentship from the UK NERC. KL was supported by a NERC fellowship (NE/L011522/1)

600 References

Aeschbacher, S., Selby, J. P., Willis, J. H. & Coop, G. (2017). Population-genomic inference of the 602 strength and timing of selection against gene flow. *Proceedings of the National Academy of Sciences of the USA,* 114, 7061-7066. https://doi.org/10.1073/pnas.1616755114

604

Ahmed, S., Compton, S. G., Butlin, R. K., & Gilmartin P. M. (2009). Wind-borne insects mediate 606 directional pollen transfer between desert fig trees 160 kilometers apart. *Proceedings of the National Academy of Sciences of the USA*, 106, 20342-20347. 608 https://doi.org/10.1073/pnas.0902213106

610 Bain, A., Borges, R. M., Chevallier, M. H., Vignes, H., Kobmoo, N., Peng, Y. Q., Cruaud, A., Rasplus, J. Y., Kjellberg, F., & Hossaert-Mckey, M. (2016). Geographic structuring into vicariant 612 species-pairs in a wide-ranging, high-dispersal plant–insect mutualism: the case of *Ficus racemosa* and its pollinating wasps. *Evolutionary Ecology*, 30, 663–684. https://doi.org/10.1007/s10682-016- 614 9836-5

616 Bankevich, A., Nurk, S., Antipov, D., Gurevich, A. A., Dvorkin, M., Kulikov, A. S. .... & Pevzner, P. A. (2012). SPAdes: a new genome assembly algorithm and its applications to single cell 618 sequencing. *Journal of Computational Biology*, 19, 455-477. https://doi.org/10.1089/cmb.2012.0021

620

Baker, C. H., Graham, G. C., Scott, K. D., Cameron, S. L., Yeates, D. K. & Merritt, D. J. (2008). 622 Distribution and phylogenetic relationships of Australian glow-worms *Arachnocampa* (Diptera, Keroplatidae)', *Molecular Phylogenetics and Evolution* 48, 506-514. https://doi.org/ 624 10.1016/j.ympev.2008.04.037

626 Bell, K. L., Moritz, C., Moussalli, A. & Yeates, D. K. (2007). Comparative phylogeography and speciation of dung beetles from the Australian Wet Tropics rainforest. *Molecular Ecology*, 16, 628 4984-4998. https://doi.org/10.1111/j.1365-294X.2007.03533.x

630 The impact of global selection on local adaptation and reproductive isolation Bisschop, G., Setter, D., Rafajlović, M., Baird, S. J. E. & Lohse, K. (2019). bioRxiv 855320. 632 https://doi.org/10.1101/855320

634 Brown, M., Cooksley, H., Carthew, S M. & Cooper, S. J. B. (2006). Conservation units and phylogeographic structure of an arboreal marsupial, the yellow-bellied glider (*Petaurus australis*). 636 *Australian Journal of Zoology*, 54, 305-317. https://doi.org/10.1071/ZO06034

638 Bryant, L. M. & Fuller, S. J. (2014). Pleistocene climate fluctuations influence phylogeographical patterns in *Melomys cervinipes* across the mesic forests of eastern Australia. *Journal of*
640 *Biogeography*, 41, 1923-1935. https://doi.org/10.1111/jbi.12341

642 Bryant, L. M. & Krosch, M. N. (2016). Lines in the land: a review of evidence for eastern Australia's major biogeographical barriers to closed forest taxa. *Biological Journal of the Linnean Society*, 119,
644 238-264. https://doi.org/10.1111/bij.12821

646 Buchfink, B., Xie, C. & Huson, D. H. (2015). Fast and sensitive protein alignment using DIAMOND. *Nature Methods,* 12, 59-60. https://doi.org/10.1038/nmeth.3176
648
Bunnefeld, L., Hearn, J., Stone, G.N. & Lohse, K. (2018). Whole genome data reveal the complex
650 history of a diverse ecological community. *Proceedings of the National Academy of Sciences of the United States of America*. 115, E6507-E6515. https://doi.org/10.1073/pnas.1800334115
652
Burke, J. M., Ladiges, P.Y., Batty, E. L., Adams, P. B., Bayly, M. J. & Katinas, L. (2013). Divergent
654 lineages in two species of *Dendrobium* orchids (*D. speciosum* and *D. tetragonum*) correspond to major geographical breaks in eastern Australia. *Journal of Biogeography*, 40, 2071-2081.
656 https://doi.org/10.1111/jbi.12145

658 Byrne, M. (2008). Evidence for multiple refugia at different time scales during Pleistocene climatic oscillations in southern Australia inferred from phylogeography. *Quaternary Science Reviews*, 27,
660 2576-2585.

662 Catullo, R. A. & Keogh, J. S. (2014). Aridification drove repeated episodes of diversification between Australian biomes: evidence from a multi-locus phylogeny of Australian toadlets
664 (*Uperoleia*: Myobatrachidae). *Molecular Phylogenetics and Evolution,* 79, 106–117. https://doi.org/10.1016/j.ympev.2014.06.012
666
Catullo, R. A., Lanfear, R., Doughty, P. & Keogh, J. S. (2014). The biogeographical boundaries of
668 northern Australia: evidence from ecological niche models and a multi-locus phylogeny of *Uperoleia* toadlets (Anura: Myobatrachidae). *Journal of Biogeography*, 41, 659–672.
670 https://doi.org/10.1111/jbi.12230

672 Chapple, D. G., Hoskin, C. J., Chapple, S. N. & Thompson, M. B. (2011). Phylogeographic divergence in the widespread delicate skink (*Lampropholis delicata*) corresponds to dry habitat
674 barriers in eastern Australia. *BMC Evolutionary Biology*, 11, 191. https://doi.org/10.1186/1471-2148-11-191
676
Chen, Y., Compton, S. G., Liu, M. & Chen, X. Y. (2012). Fig trees at the northern limit of their
678 range: the distributions of cryptic pollinators indicate multiple glacial refugia. *Molecular Ecology*, 21, 1687-1701. https://doi.org/10.1111/j.1365-294X.2012.05491.x
680
Clark, P. U., Hostetler, S. W., Pisias, N. G., Schmittner A. & Meissner, K. J. (2007). Mechanisms
682 for an ~7-Kyr climate and sea-level oscillation during marine isotope stage 3. In: *Ocean Circulation: Mechanisms and Impacts—Past and Future Changes of Meridional Overturning*.
684 American Geophysical Union. Geophysical Monograph Series, Volume 173. https://doi.org/10.1029/173GM15
686
Cook, James M. & Rasplus, J.-Y. (2003). Mutualists with attitude: coevolving fig wasps and figs.
688 *Trends in Ecology & Evolution*, 18, 241-248. https://doi.org/10.1016/S0169-5347(03)00062-4

690 Cooper, L., Bunnefeld, L., Hearn, J., Cook, J. M., Lohse, K. & Stone, G. N. (2020)a. Phylogeography of *Pleistodontes nigriventris* from northern and southern populations in Australia.
692 Sequence read data in the European Nucleotide Archive, Study PRJEB35527. Available from https://www.ebi.ac.uk/ena/browser/view/PRJEB35527

694

Cooper, L., Bunnefeld, L., Hearn, J., Cook, J. M., Lohse, K. & Stone, G. N. (2020)b. 696 Phylogeography of *Pleistodontes nigriventris* from northern and southern populations in Australia. Trimmed sequence block data and associated *Mathematica* notebook for blockwise analyses. 698 Available from the Dryad Digital Repository, doi:// (to be added on acceptance).

700

DePristo, M. A., Banks, E., Poplin, R., Garimella, K. V., Maguire, J. R., Hartl, C. ... & Daly, M. J. 702 (2011). A framework for variation discovery and genotyping using next-generation DNA sequencing data. *Nature Genetics*, 43, 491-498. https://doi.org/10.1038/ng.806

704

Dixon, D. J. (2003). A taxonomic revision of the Australian *Ficus* species in the section 706 Malvanthera (*Ficus* subg. *Urostigma*: Moraceae). *Telopea*, 10, 125-153. https://doi.org/10.7751/telopea20035611

708

Dolman, G. & Moritz, C. (2006). A multilocus perspective on refugial isolation and divergence in 710 rainforest skinks (*Carlia*). *Evolution*, 60, 573-582. https://doi.org/10.1554/05-487.1

712 Durand E. Y., Patterson N., Reich D., & Slatkin, M. (2011). Testing for ancient admixture between closely related populations. *Molecular Biology and Evolution,* 28, 2239–2252. . 714 https://doi.org/10.1093/molbev/msr048

716 Felsenstein, J. 2003. *Inferring Phylogenies*. Sinauer, 664pp.

718 Frankham, G. J., Handasyde, K. A. & Eldridge, M. D. B (2016). Evolutionary and contemporary responses to habitat fragmentation detected in a mesic zone marsupial, the long-nosed potoroo 720 (*Potorous tridactylus*) in south-eastern Australia. *Journal of Biogeography*, 43, 653-665. https://doi.org/10.1111/jbi.12659

722

García-Alcalde, F., Okonechnikov, K., Carbonell, J., Cruz, L. M., Götz, S., Tarazona, S., Dopazo, 724 J., Meyer, T. F. & Conesa, A. (2012). Qualimap: evaluating next-generation sequencing alignment data. *Bioinformatics*, 28, 2678–2679. https://doi.org/10.1093/bioinformatics/bts503

726

Greeff, J. M., van Vuuren, G. J. J., Kryger, P. & Moore, J. C. (2009). Outbreeding and possibly 728 inbreeding depression in a pollinating fig wasp with a mixed mating system. *Heredity*, 102, 349-356. https://doi.org/10.1038/hdy.2009.2

730

Haine, E. R., & Cook, J. M. (2005). Convergent incidences of *Wolbachia* infection in fig wasp 732 communities from two continents. *Proceedings of the Royal Society of London, Series B Biological Sciences*, 272, 421-429. https://doi.org/10.1098/rspb.2004.2956

734

Hare, M. P. (2001). Prospects for nuclear gene phylogeography. *Trends in Ecology & Evolution*, 736 16, 700-706. https://doi.org/10.1016/S0169-5347(01)02326-6

738 Harrison, R. D. (2003). Fig wasp dispersal and the stability of a keystone plant resource in Borneo. *Proceedings of the Royal Society of London, Series B Biological Sciences*, 270, Suppl 1: S76-9.

740

Harrison, R.D. (2005) Figs and the diversity of tropical rainforests. *Bioscience* 55, 1053-1064. 742 https://doi.org/10.1098/rsbl.2003.0018

744 Harrison, R. D. & Rasplus, J.-Y. (2006). Dispersal of fig pollinators in Asian tropical rain forests. *Journal of Tropical Ecology*, 22, 631-639. https://doi.org/10.1017/S0266467406003488

746

Hearn, J., Stone, G. N., McInnes, L., Nicholls, J. A., Barton, N. H. & Lohse, K. (2014). Likelihood-748 based inference of population history from low coverage de novo genome assemblies. *Molecular Ecology* 23, 198-211. https://doi.org/10.1111/mec.12578.

750

Hey, J. & Nielsen, R. (2004). Multilocus methods for estimating population sizes, migration rates and divergence time, with applications to the divergence of *Drosophila pseudoobscura* and *D. persimilis*. *Genetics*, 167, 747-60. https://doi.org/10.1534/genetics.103.024182.

Hocknull, S. A., Zhao, J.-X., Feng, Y.-X. & Webb, G. E. (2007). Responses of Quaternary rainforest vertebrates to climate change in Australia. *Earth and Planetary Science Letters*, 264, 317-331. https://doi.org/10.1016/j.epsl.2007.10.004

Jennings, W. B. & Edwards, S. V. (2005). Speciational history of Australian grass finches (*Poephila*) inferred from thirty gene trees. *Evolution*, 59, 2033-2047. https://doi.org/10.1111/j.0014-3820.2005.tb01072.x

Jermiin, L. S. & Crozier, R. H. (1994). The cytochrome b region in the mitochondrial DNA of the ant *Tetraponera rufoniger*: sequence divergence in Hymenoptera may be associated with nucleotide content. Journal of Molecular Evolution, 38, 282-294. https://doi.org/10.1007/BF00176090

Jesus, F. F., Wilkins, J. F., Solferini, V. N. & Wakeley, J. (2006). Expected coalescence times and segregating sites in a model of glacial cycles. *Genetic and Molecular Research*, 5, 466-474.

Keightley, P. D., Ness, R. W., Halligan, D. L. & Haddrill, P. R. (2014). Estimation of the spontaneous mutation rate per nucleotide site in a *Drosophila melanogaster* full-sib family. *Genetics*, 196, 313-320. https://doi.org/10.1534/genetics.113.158758

Keightley, P. D., Pinharanda, A., Ness, R. W., Simpson, F., Dasmahapatra, K. K., Mallet, J., Davey, J. W. & Jiggins C. D. (2015). Estimation of the spontaneous mutation rate in *Heliconius melpomene*. *Molecular Biology and Evolution*, 32, 239-243. https://doi.org/10.1093/molbev/msu302

Kelleher, J., Etheridge, A. M. & McVean, G. (2016). Efficient coalescent simulation and genealogical analysis for large sample sizes. *PLoS Computational Biology*, 12, e1004842. https://doi.org/10.1371/journal.pcbi.1004842 https://doi.org/10.1371/journal.pcbi.1004842

Kershaw, A. P. (1994). Pleistocene vegetation of the humid tropics of northeastern Queensland, Australia. *Paleoclimatology, Paleogeography, Paleoecology*, 109, 399–412. https://doi.org/10.1016/0031-0182(94)90188-0 https://doi.org/10.1016/0031-0182(94)90188-0

Kobmoo, N., Hossaert-McKey, M., Rasplus, J.-Y. & Kjellberg, F. (2010). *Ficus racemosa* is pollinated by a single population of a single agaonid wasp species in continental South-East Asia. *Molecular Ecology*, 19, 2700-2712. https://doi.org/10.1111/j.1365-294X.2010.04654.x

Kumar, S., Jones, M., Koutsovoulos, G., Clarke, M. & Blaxter, M. (2013). Blobology: exploring raw genome data for contaminants, symbionts and parasites using taxon-annotated GC-coverage plots', *Frontiers in Genetics*, 4, 237. https://doi.org/10.3389/fgene.2013.00237

Langmead, B., & Salzberg, S. L. (2012). Fast gapped-read alignment with Bowtie 2. *Nature Methods*, 9, 357-359. https://doi.org/10.1038/nmeth.1923

Lanier, H. C., & Knowles, L. L.(2012). Is recombination a problem for species-tree analyses? *Systematic Biology*, 61, 691-701. https://doi.org/10.1093/sysbio/syr128

Li, H. (2011). A statistical framework for SNP calling, mutation discovery, association mapping and population genetical parameter estimation from sequencing data. *Bioinformatics*, 27, 2987-2993. https://doi.org/10.1093/bioinformatics/btr509

Li, H. & Durbin, R. (2009). Fast and accurate short read alignment with Burrows-Wheeler transform. *Bioinformatics*, 25, 1754-1760. https://doi.org/10.1093/bioinformatics/btp324

Li, H. & Durbin, R. (2011). Inference of human population history from individual whole-genome sequences. *Nature*, 475, 493-496. https://doi.org/10.1038/nature10231

Li, H., Handsaker, B., Wysoker, A., Fennell, T., Ruan, J., Homer, N., Marth, G., Abecasis, G., Durbin, R. & Subgroup Genome Project Data Processing. (2009). The Sequence Alignment/Map format and SAMtools. *Bioinformatics*, 25, 2078-2079. https://doi.org/10.1093/bioinformatics/btp352

Liu, M., Compton, S. G., Peng, F. E., Zhang, J. & Chen, X. Y. (2015). Movements of genes between populations: are pollinators more effective at transferring their own or plant genetic markers?', *Proceedings of the Royal Society of London, Series B Biological Sciences,* 282, 20150290. https://doi.org/10.1098/rspb.2015.0290

Lohse, K., Chmelik, M., Martin, S. H. & Barton, N. H. (2016). Efficient strategies for calculating blockwise likelihoods under the coalescent. *Genetics*, 202, 775-786. https://doi.org/10.1534/genetics.115.183814

Lohse, K. & Frantz, L. A. F. (2014). Neandertal admixture in Eurasia confirmed by maximum-likelihood analysis of three genomes. *Genetics,* 196, 1241-1251. https://doi.org/10.1534/genetics.114.162396

Lohse, K., Harrison, R. J. & Barton, N. H. (2011). A general method for calculating likelihoods under the coalescent process. *Genetics*, 189, 977-987. https://doi.org/10.1534/genetics.111.129569

Lopez-Vaamonde, C., Rasplus, J.Y., Weiblen, G.D., and Cook, J.M. (2001) Molecular phylogenies of fig wasps: Partial cocladogenesis of pollinators and parasites. *Molecular Phylogenetics and Evolution*' 21, 55-71. https://doi.org/10.1006/mpev.2001.0993

Lopez-Vaamonde, C., Dixon, D. J., Cook, J. M. & Rasplus, J.-Y. (2002). Revision of the Australian species of *Pleistodontes* (Hymenoptera: Agaonidae) fig-pollinating wasps and their host-plant associations. *Zoological Journal of the Linnean Society*, 136, 637-683. https://doi.org/10.1046/j.1096-3642.2002.00040.x

Macqueen, P., Seddon, J. M., Austin, J. J., Hamilton, S. & Goldizen, A. W. (2010). Phylogenetics of the pademelons (Macropodidae: *Thylogale*) and historical biogeography of the Australo-Papuan region. *Molecular Phylogenetics and Evolution*, 57, 1134-1148. https://doi.org/10.1016/j.ympev.2010.08.010

Macqueen, P., Seddon, J. M. & Goldizen, A. W. (2012). Effects of historical forest contraction on the phylogeographic structure of Australo-Papuan populations of the red-legged pademelon (Macropodidae: *Thylogale stigmatica*). *Austral Ecology*, 37, 479-490. https://doi.org/10.1111/j.1442-9993.2011.02309.x

Maldonado, S. P., Melville, J., Peterson, G. N. L. & Sumner, J. (2012). Human-induced versus historical habitat shifts: identifying the processes that shaped the genetic structure of the threatened grassland legless lizard, *Delma impar*. *Conservation Genetics*, 13, 1329-1342. https://doi.org/10.1007/s10592-012-0377-3

Male, T. D. & Roberts, G. E. (2005). Host associations of the strangler fig *Ficus watkinsiana* in a subtropical Queensland rain forest. Austral Ecology, 30, 229-236. https://doi.org/10.1111/j.1442-9993.2005.01442.x

Markgraf, V., McGlone, M. & Hope, G. (1995). Neogene paleoenvironmental and paleoclimatic change in southern temperate ecosystems — a southern perspective. *Trends in Ecology & Evolution*, 10, 143-147. https://doi.org/10.1016/S0169-5347(00)89023-0

Martin, H. A. (2006). Cenozoic climatic change and the development of the arid vegetation in Australia. *Journal of Arid Environments*, 66, 533-563. https://doi.org/10.1016/j.jaridenv.2006.01.009

Martin, M. (2011). Cutadapt removes adapter sequences from high-throughput sequencing reads. *EMBnet.journal*, 17, No 1: Next Generation Sequencing Data Analysis. https://doi.org/https://doi.org/10.14806/ej.17.1.200

Martin, S. H., Dasmahapatra, K. K., Nadeau, N. J., Salazar, C., Walters, J. R., Simpson, F., Blaxter, M., Manica, A., Mallet, J. & Jiggins, C. D. (2013). Genome-wide evidence for speciation with gene flow in *Heliconius* butterflies. *Genome Research*, 23, 1817-1828. https://doi.org/10.1101/gr.159426.113

McGuigan, K., McDonald, K., Parris, K. & Moritz, C. (1998). Mitochondrial DNA diversity and historical biogeography of a wet forest-restricted frog (*Litoria pearsoniana*) from mid-east Australia. *Molecular Ecology*, 7, 175-186. https://doi.org/10.1046/j.1365-294x.1998.00329.x

McKenna, A., Hanna, M., Banks, E., Sivachenko, A., Cibulskis, K., Kernytsky, A., Garimella, K., Altshuler, D., Gabriel, S., Daly, M. & DePristo, M. A. (2010). The Genome Analysis Toolkit: a MapReduce framework for analyzing next generation DNA sequencing data, *Genome Research*, 20, 1297-1303. https://doi.org/10.1101/gr.107524.110

Nicholls, J. A., & Austin, J. J. (2005). Phylogeography of an east Australian wet forest bird, the satin bowerbird (*Ptilonorhynchus violaceus*), derived from mtDNA, and its relationship to morphology. *Molecular Ecology*, 14, 1485-1496. https://doi.org/10.1111/j.1365-294X.2005.02544.x

Nielsen, R. & Wakeley, J. (2001). Distinguishing migration from isolation: a Markov Chain Monte Carlo approach.*Genetics*,158, 885-896

Niu, L.-H., Song, X.-F., He, S. M., Zhang, P., Wang, N. X., Li, Y. & Huang, D. W. (2015). New insights into the fungal community from the raw genomic sequence data of fig wasp *Ceratosolen solmsi*. *BMC Microbiology*, 15, 27. https://doi.org/10.1186/s12866-015-0370-3

Nürnberger, B., Lohse, K., Fijarczyk, A., Szymura, J. M. & Blaxter, M. L. (2016). Para-allopatry in hybridizing fire-bellied toads (*Bombina bombina* and *B. variegata*): inference from transcriptome-wide coalescence analyses. *Evolution*, 70, 1803-1818. https://doi.org/10.1111/evo.12978

Okonechnikov, K., Conesa, A. & García-Alcalde, F (2016). Qualimap 2: advanced multi-sample quality control for high-throughput sequencing data. *Bioinformatics*, 32, 292–294. https://doi.org/10.1093/bioinformatics/btv566

Oswald, J. A., Overcast, I., Mauck, W. M., Andersen, M. J. & Smith, B. T. (2017). Isolation with asymmetric gene flow during the nonsynchronous divergence of dry forest birds. *Molecular Ecology*, 26, 1386-1400. https://doi.org/10.1111/mec.14013

Pope, L. C., Estoup, A. & Moritz, C. (2000). Phylogeography and population structure of an ecotonal marsupial, *Bettongia tropica*, determined using mtDNA and microsatellites. *Molecular Ecology*, 9, 2041-2053. https://doi.org/10.1046/j.1365-294x.2000.01110.x

Pope, L. C., Storch, D., Adams, M., Moritz, C. & Gordon, G. (2001). A phylogeny for the genus *Isoodon* and a range expansion *for I. obesulus peninsulae* based on mtDNA control region and morphology. *Australian Journal of Zoology*, 49, 411-434. https://doi.org/10.1071/ZO00060

Price, A. L., Jones, N. C. & Pevzner, P. A. (2005). *De novo* identification of repeat families in large genomes. *Bioinformatics*, 21 Suppl 1, i351-i358. https://doi.org/10.1093/bioinformatics/bti1018

Quinlan, A. R. & Hall, I. M. (2010). BEDTools: a flexible suite of utilities for comparing genomic features, Bioinformatics, 26, 841-842. https://doi.org/10.1093/bioinformatics/btq033

Ringbauer, H., Kolesnikov, A., Field, D. L. & Barton, N. H. (2018). Estimating barriers to gene flow from distorted isolation-by-distance patterns. *Genetics*, 208, 1231-1245. https://doi.org/10.1534/genetics.117.300638

Rix, M. G. & Harvey, M. S. (2012). Phylogeny and historical biogeography of ancient assassin spiders (Araneae: Archaeidae) in the Australian mesic zone: evidence for Miocene speciation within Tertiary refugia. *Molecular Phylogenetics and Evolution*, 62, 375-396. https://doi.org/10.1016/j.ympev.2011.10.009

Rodriguez, L. J., Bain, A., Chou, L.-S., Conchou, L., Cruaud, A., Gonzales, R., Hossaert-McKey, M., Rasplus, J.-Y., Tzeng, H.-Y. & Kjellberg, F. (2017). Diversification and spatial structuring in the mutualism between *Ficus septica* and its pollinating wasps in insular South East Asia. *BMC Evolutionary Biology*, 17, 207. https://doi.org/10.1186/s12862-017-1034-8

Rønsted, N., Weiblen, G. D., Savolainen, V. & Cook, J. M. (2008). Phylogeny, biogeography, and ecology of *Ficus* section Malvanthera (Moraceae). *Molecular Phylogenetics and Evolution*, 48, 12-22. https://doi.org/10.1016/j.ympev.2008.04.005

Schiffer, M., Kennington, W. J., Hoffmann, A. A. & Blacket, M. J. (2007). Lack of genetic structure among ecologically adapted populations of an Australian rainforest *Drosophila* species as indicated by microsatellite markers and mitochondrial DNA sequences. *Molecular Ecology*, 16, 1687-700. . https://doi.org/10.1111/j.1365-294X.2006.03200.x

Schäuble, C. S., & Moritz, C. (2001). Comparative phylogeography of two open forest frogs from eastern Australia. *Biological Journal of the Linnean Society*, 74, 157-70. https://doi.org/10.1111/j.1095-8312.2001.tb01384.x

Schneider, C. J., Cunningham, M. & Moritz, C. (1998). Comparative phylogeography and the history of endemic vertebrates in the Wet Tropics rainforests of Australia. *Molecular Ecology*, 7, 487-498. https://doi.org/10.1046/j.1365-294x.1998.00334.x

Segar, S. T., Dunn, D. W., Darwell, C. T. & Cook, J. M. (2014). How to be a fig wasp down under: the diversity and structure of an Australian fig wasp community. *Acta Oecologica*, 57, 17-27. https://doi.org/10.1016/j.actao.2013.03.014

Siddall, M., Rohling, E. J., Thompson, W. G. & Waelbroeck, C. (2008). Marine isotope stage 3 sea level fluctuations: data synthesis and new outlook. *Reviews of Geophysics*, 46. https://doi.org/10.1029/2007RG000226

Simao, F. A., Waterhouse, R. M., Ioannidis, P., Kriventseva, E. V. & Zdobnov, E. M. (2015). BUSCO: assessing genome assembly and annotation completeness with single-copy orthologs. *Bioinformatics*, 31, 3210-3212. https://doi.org/10.1093/bioinformatics/btv351

Smissen, P. J., Melville, J., Sumner, J. & Jessop, T. S. (2013). Mountain barriers and river conduits: phylogeographical structure in a large, mobile lizard (Varanidae: *Varanus varius*) from eastern Australia. *Journal of Biogeography*, 40, 1729–1740. https://doi.org/10.1111/jbi.12128

Smit, A. F. A., Hubley, R. & Green, P. (2013-2015). *RepeatMasker Open-4.0*. 2013-2015 <http://www.repeatmasker.org>.

Sousa, V. & Hey, J. (2013). Understanding the origin of species with genome-scale data: modelling gene flow. *Nature Reviews Genetics*, 14, 404–414. https://doi.org/10.1038/nrg3446

Strasburg, J. L., & Rieseberg, L. H. (2010). How robust are “Isolation with Migration” analyses to violations of the IM model? A simulation Study. *Molecular Biology and Evolution*, 27, 297-310. https://doi.org/10.1093/molbev/msp233

978 Stuart-Fox, D. M., Schneider, C. J., Moritz, C. & Couper, P. J. (2001). Comparative phylogeography of three rainforest restricted lizards from mid-east Queensland. *Australian Journal*
980 *of Zoology*, 49, 119–127. https://doi.org/10.1071/ZO00092

982 Stumpf, M. P. & McVean, G. A. (2003). Estimating recombination rates from population-genetic data. *Nature Reviews Genetics*, 4, 959-68. https://doi.org/10.1038/nrg1227
984
Sutton, T. L., Riegler, M. & Cook, J. M. (2016). One step ahead: a parasitoid disperses farther and
986 forms a wider geographic population than its fig wasp host. *Molecular Ecology*, 25, 882-94. https://doi.org/10.1111/mec.13445
988
Treangen, T. J. & Salzberg, S. L. (2011). Repetitive DNA and next-generation sequencing:
990 computational challenges and solutions. *Nature Reviews Genetics*, 13, 36-46. https://doi.org/10.1038/nrg3117
992
Van der Auwera, G. A., Carneiro, M. O., Hartl, C., Poplin, R., Del Angel, G., Levy-Moonshine, A., ...
994 DePristo, M. A. (2013). From FastQ data to high confidence variant calls: the Genome Analysis Toolkit best practices pipeline. *Current Protocols in Bioinformatics*, 43, 11.10.1-33.
996 https://doi.org/10.1002/0471250953.bi1110s43.

998 Van Meerbeeck, C. J., Renssen, H. & Roche, D. M. (2009). How did Marine Isotope Stage 3 and Last Glacial Maximum climates differ? – Perspectives from equilibrium simulations. *Climate of the*
1000 *Past*, 5, 33-51. https://doi.org/10.5194/cp-5-33-2009

1002 Wachi, N., Kusumi, J., Tzeng, H. Y. & Su, Z. H. (2016). Genome-wide sequence data suggest the possibility of pollinator sharing by host shift in dioecious figs (Moraceae, *Ficus*). *Molecular Ecology*,
1004 25, 5732-5746. https://doi.org/10.1111/mec.13876

1006 Wall, J. D. (2003). Estimating ancestral population sizes and divergence times. *Genetics*, 163, 395-404.
1008
Wang, Z. & Liu, K. J. (2016). A performance study of the impact of recombination on species tree
1010 analysis. *BMC Genomics*, 17, 785. https://doi.org/10.1186/s12864-016-3104-5

1012 Ware, A. B. & Compton, S. G. (1994)a. Dispersal of adult female fig wasps. 1. Arrivals and departures. *Entomologia Experimentalis et Applicata*, 73, 221–229. https://doi.org/10.1111/j.1570-
1014 7458.1994.tb01859.x

1016 Ware, A. B. & Compton, S. G. (1994)b. Dispersal of adult female fig wasps. 2. Movements between trees. *Entomologia Experimentalis et Applicata,* 73, 231–238.
1018 https://doi.org/10.1111/j.1570-7458.1994.tb01860.x

1020 Weber, L. C., Van der Wal, J., Schmidt, S., McDonald, W. J. F., Shoo, L. P. & Ladiges, P. (2014). Patterns of rain forest plant endemism in subtropical Australia relate to stable mesic refugia and
1022 species dispersal limitations. *Journal of Biogeography*, 41, 222-38. https://doi.org/10.1111/jbi.12219
1024
Werren, J. H., Richards, S., Desjardins, C. A., Niehuis, O., Gadau, J. & Colbourne, J. K. (2010).
1026 Functional and evolutionary insights from the genomes of three parasitoid *Nasonia* species. *Science*, 327, 343-348. https://doi.org/10.1126/science.1178028
1028
Xiao, J. H., Yue, Z., Jia, L. Y., Yang, X. H., Niu, L. H., Wang, Z., ... Huang, D. W. (2013). Obligate
1030 mutualism within a host drives the extreme specialization of a fig wasp genome. *Genome Biology*, 14, R141. https://doi.org/10.1186/gb-2013-14-12-r141
1032

Yang, L. Y., Machado, C. A., Dang, X. D., Peng, Y. Q., Yang, D. R., Zhang, D. Y. & Liao, W. J. (2015). The incidence and pattern of co-pollinator diversification in dioecious and monoecious figs. *Evolution*, 69, 294-304. https://doi.org/10.1111/evo.12584

Yu, H., Tian, E. W., Zheng, L. N., Deng, X. X., Cheng, Y. F., Chen, L. F. ... & Kjellberg, F. (2019) Multiple parapatric pollinators have radiated across a continental fig tree displaying clinal genetic variation. *Molecular Ecology,* 28, 2391-2405. https://doi.org/10.1111/mec.15046

Zerbino, D. R. & Birney, E. (2008). Velvet: algorithms for *de novo* short read assembly using de Bruijn graphs. *Genome Research*, 18, 821-9. https://doi.org/10.1101/gr.074492.107

Zhang, J., Kobert, K., Flouri, T. & Stamatakis, A. (2014). PEAR: a fast and accurate Illumina Paired-End reAd mergeR. *Bioinformatics*, 30, 614-620. https://doi.org/10.1093/bioinformatics/btt593

Data Accessibility

The short read data have been deposited at the ENA short read archive (number PRJEB35527).

CO1 barcode sequences for the four *Pleistodontes nigriceps* individuals have been deposited in Genbank: N1 MF597824; N2 MF597800; S1 MF597825; S2 MF597826).

The *Mathematica* notebook and blockwise sequence data for this study are available from the Dryad repository, doi: (added on acceptance).

Author contributions.

LC, GNS, KL and JMC designed the research. LC, LB, KL and JH performed the research and analysed the data. GNS, KL and LC wrote the paper, with editorial input from all authors.

Table 1. Maximum composite likelihood estimates (MCLE) of model support and demographic parameters under (a) IM and (b) ADM models. The best supported model is highlighted in bold with parameter 95% confidence intervals estimated by parametric bootstrap. n(N_e) indicates the number of population size parameters in the model, and N_a indicates the population(s) retaining the ancestral population size. Mig indicates the direction of gene flow in the model, with 0 indicating a model with no gene flow. Model support is measured relative to the best fit model in each class (IM9 in (a) and ADM10 in (b)). Likelihood ratio tests (LRT) were calculated as 2ΔlnL.

(a) IM (Isolation with migration) models

Model	n(N_e)	*Na*	Mig	ΔlnL	LRT	*T*	*B*	*M*
IM1	1	both	0	-22,877	n/a	3.938	n/a	n/a
IM2	1	both	N->S	-5,078	35,598	5.210	n/a	0.044
IM3	1	both	S->N	-1,122	43,509	5.533	n/a	0.057
IM4	2	N	0	-22,740	274	3.523	1.198	n/a
IM5	2	S	0	-21,298	3,157	3.808	1.055	n/a
IM6	2	N	N->S	-2,855	36,885	6.417	0.774	0.051
IM7	2	N	S->N	-500	44,479	6.193	0.872	0.061
IM8	2	S	N->S	-1,757	39,081	4.573	1.348	0.065
IM9	**2**	**S**	**S->N**	**0**	**45,481**	**5.137 (4.784-5.489)**	**1.193 (1.089-1.296)**	**0.071 (0.045-0.097)**
IM9 sim						0.299	5.150	1.197

(b) ADM (Instantaneous admixture) models

Model	n(N_e)	N_a	Mig	ΔlnL	LRT	Tadm	T	B	f
ADM1	1	both	0	-6,349	37,230	n/a	4.969	n/a	0.015
ADM2	1	both	0	-6,349	37,230	n/a	4.969	n/a	0.015
ADM3	1	both	N->S	-4,995	2,634	2.194	6.122	n/a	0.296
ADM4	1	both	S->N	-1,110	10,478	1.970	6.095	n/a	0.257
ADM5	2	N	0	-6,536	36,583	n/a	4.193	1.313	0.014
ADM6	2	S	0	-5,632	35,508	n/a	4.631	1.152	0.017
ADM7	2	N	N->S	-1,645	9,784	1.642	5.195	1.329	0.257
ADM8	2	N	S->N	-172	10,919	2.003	6.872	0.857	0.256
ADM9	2	S	N->S	-1975	9,122	2.281	7.276	0.767	0.291
ADM10	**2**	**S**	**S->N**	**0**	**11,263**	**1.656 (1.509-1.802)**	**5.643 (5.317-5.966)**	**1.181 (1.093-1.269)**	**0.239 (0.206-0.272)**
ADM10 sim						0.302	1.653	5.604	1.184

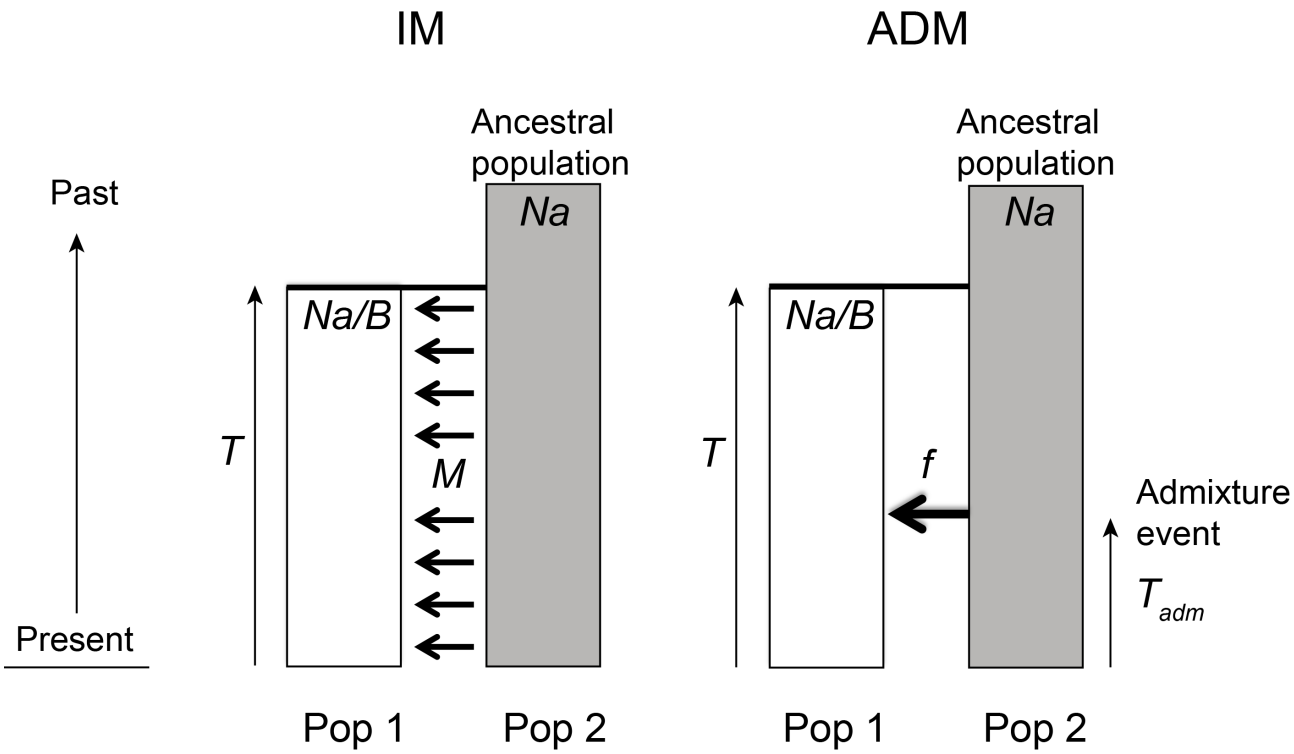

Figure 1. The IM (divergence with continuous migration) and ADM (divergence with instantaneous admixture) models of population divergence with gene flow, showing the demographic parameters estimated in our blockwise method analyses. Gene flow can be modelled in either direction. *Na* represents the size of an ancestral population extending back into the past that splits into two daughter populations at time *T* (scaled by 2*Ne*) generations. One population retains the same population size *Na,* and one is free to have a new population size *Na*/*B,* where *B* is a scaling factor. Post divergence gene flow in the IM model is a continuous process with total *M* per generation = *4Ne* * *m,* where m is the individual migration rate per generation. In the ADM model, gene flow is modelled as an instantaneous admixture event at time T_{adm} (scaled by 2Ne) generations ago, at which a fraction *f* of lineages in the source population are transferred to the receiving population.

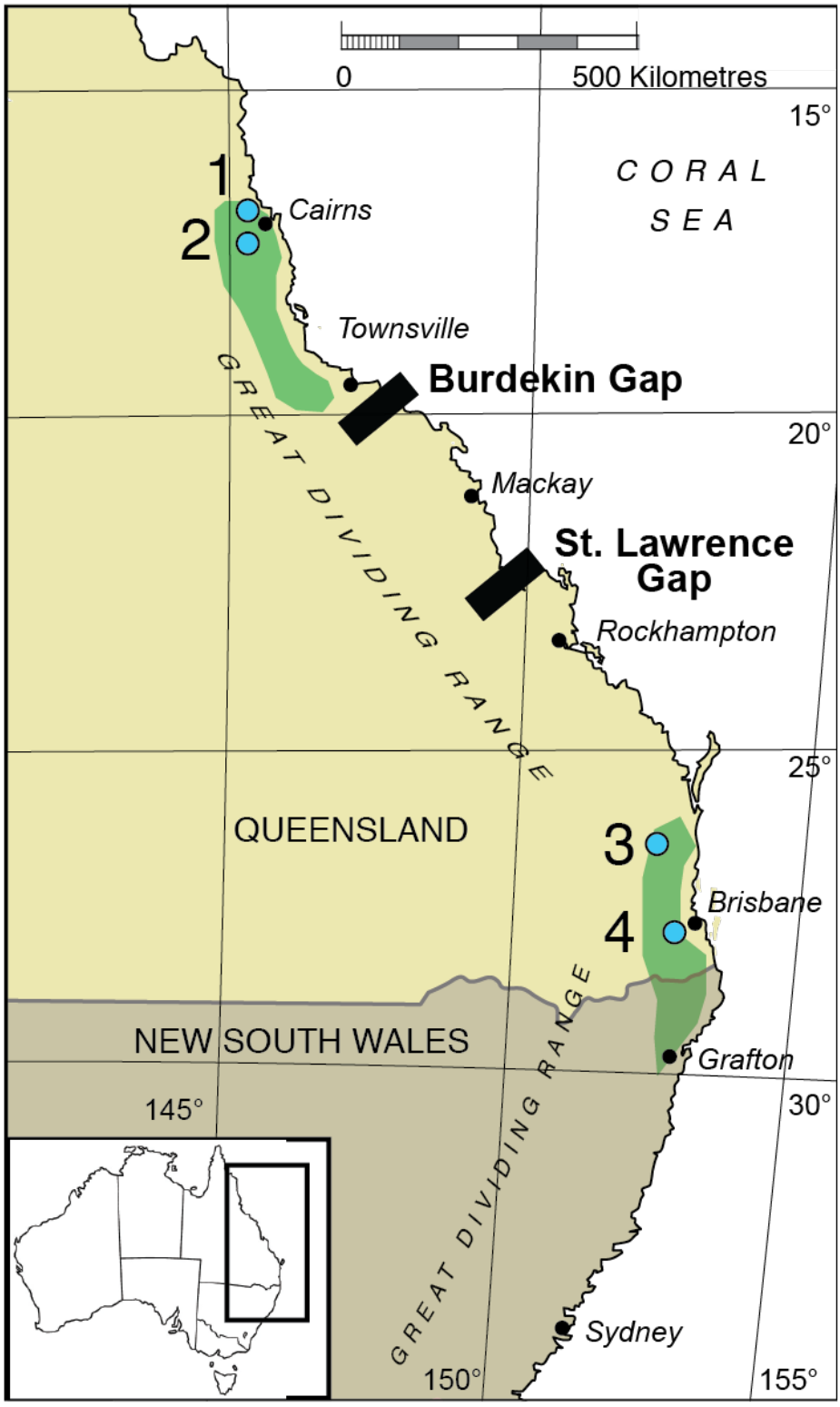

Figure 2. Map of the east coast of Australia, showing the distribution of Ficus watkinsiana (green) (after Dixon (2003)), the Burdekin and St. Lawrence Gaps (black), and the four sample sites (blue circles). The two Northern sampling sites are Kamerunga (1) and Kairi (2); the two Southern sites are Settlers Rise (3) and Main Range (4). The location of the study region within the whole of Australia is shown by the box in the inset at bottom left.

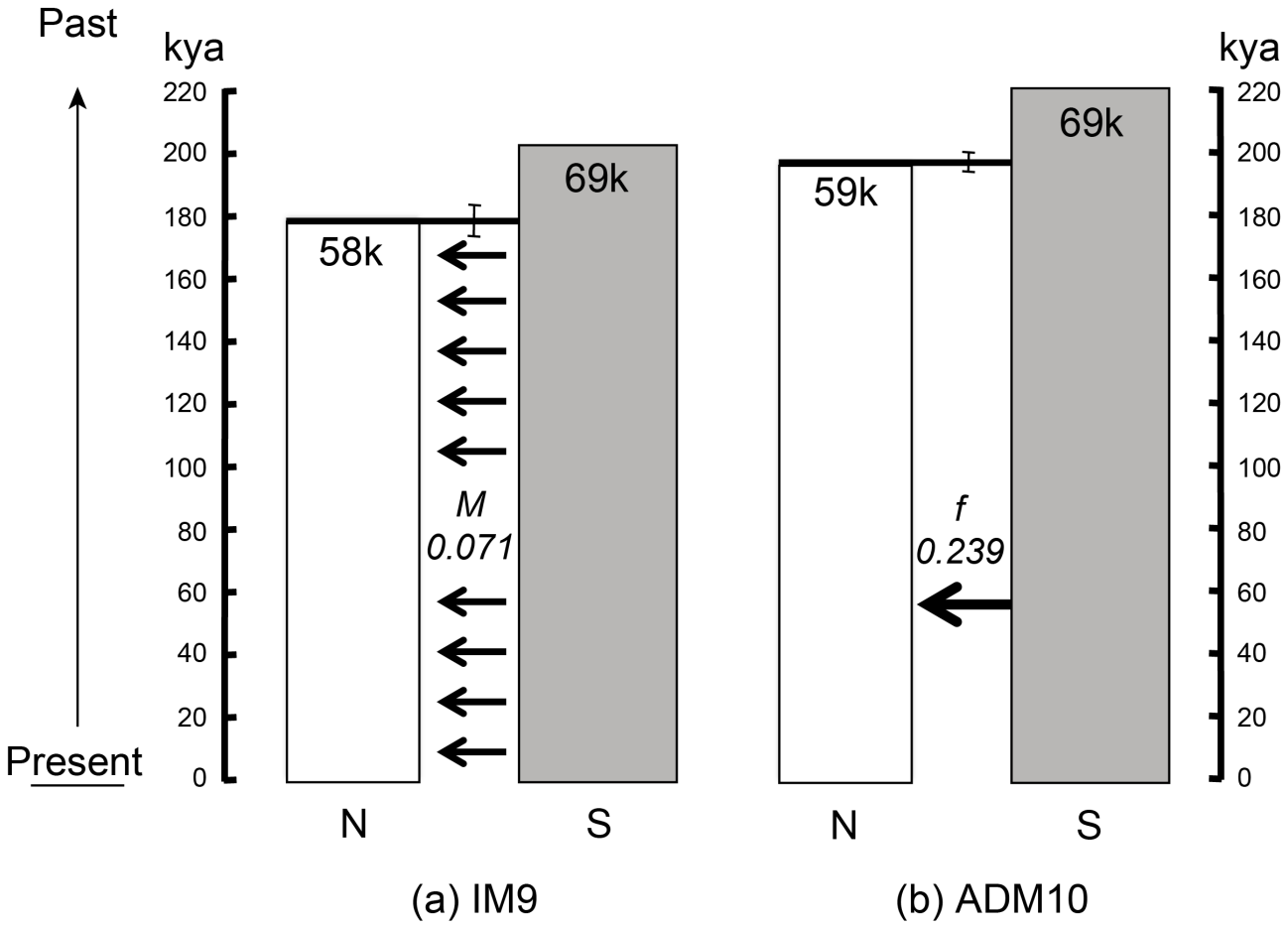

Figure 3. The best supported models under (a) IM and (b) ADM scenarios for *Pleistodontes nigriventris.* Bars joining the populations at divergence are the 95% confidence intervals for the divergence time. The time is measured in thousands of years. The population widths are scaled according to their population size estimates (given in thousands). 95% confidence intervals for other parameters are given in Table 1.

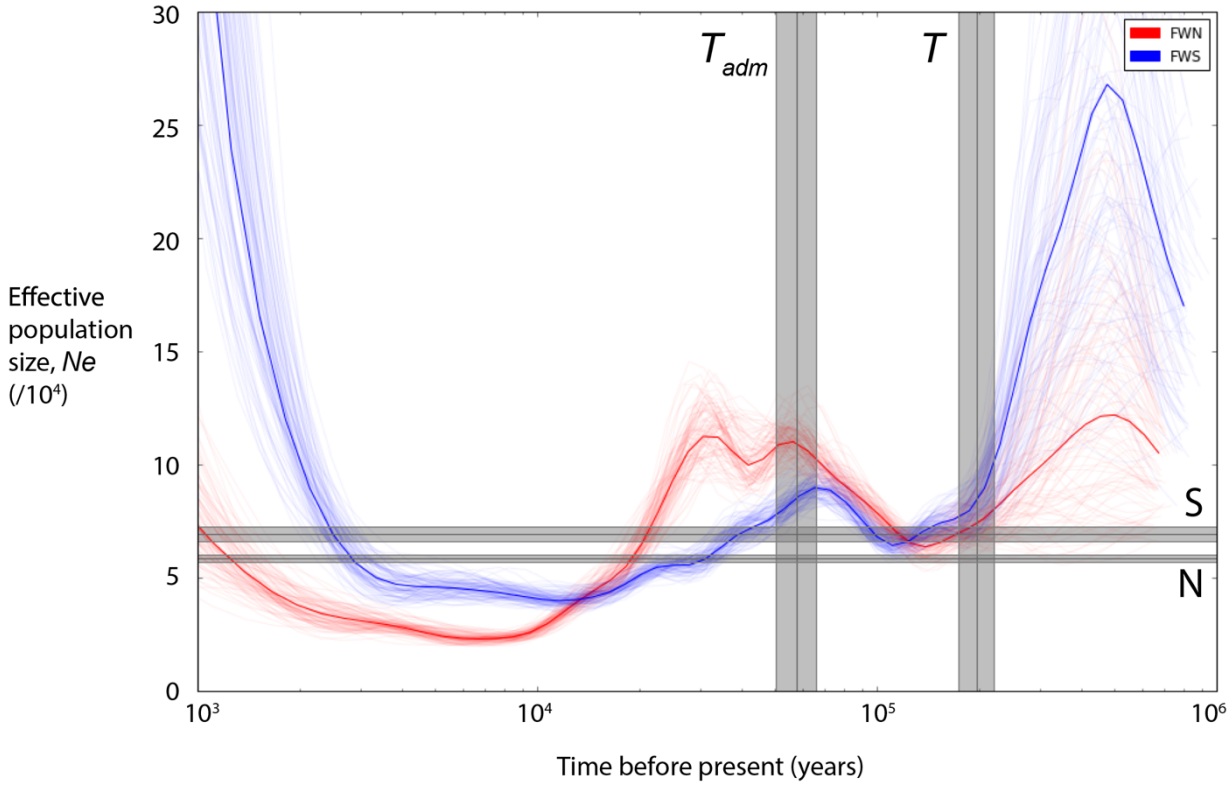

Figure 4. Population size trajectories for the Northern (red) and Southern (blue) populations inferred using PSMC. Heavy red and blue lines represent estimates for each population, thin lines show individual bootstrap replicates. Maximum composite likelihood estimate (MCLE) for the population sizes for the North and South populations and the dates of admixture (*Tadm*) and population divergence (*T*) under the model that gives the best fit to the blockwise data (ADM10) (and their 95% confidence intervals) are overlaid in grey.